# Calculations of Emittance and Damping Time Effects in the SLC Damping Rings*

## T. Limberg, H. Moshammer, T. Raubenheimer, J. Spencer, R. Siemann

Stanford Linear Accelerator Center, Stanford University, Stanford, CA 94309 USA

### Abstract

In a recent NDR machine experiment the transverse emittance was studied as a function of store time and tune. To explain the observed transverse emittance damping time constants, the magnetic measurement data of the longitudinal field of the bending magnets had to be taken into account. The variation of the transverse emittances with tune due to misalignments and the associated anomalous dispersion is studied as well as the effect of synchrobetatron coupling due to dispersion in the RF cavities.

### Introduction

Damping rings reduce the transverse phase space of electron and positron beams to suitably small values near the injector so that the bunches can collide with high luminosity. The Stanford Linear Collider (SLC) operates at 120 Hz (60 Hz at long store) and electron bunches stay for about 2 (4) damping times in the North Damping Ring (NDR). Any deviation from the design equilibrium emittance or design damping time may degrade the performance of the Collider.

We recalculate the theoretically expected transverse damping time constants using the measured field of the bending magnet. Experimental data show a tune dependance of the emittance in the damping ring [1]. We investigate two potential sources of this tune dependence: (a) random misalignments of magnets which increase the emittance and disturb the lattice functions and (b) synchrobetatron coupling caused by dispersion at the RF cavities.

## I. Emittances and Damping for Different Bending Magnet Models

We compare hard edge (the field at the ends of the magnet rises from zero to the peak value discontinuously) and soft edge models using the magnetic measurement data of the dipole fringe fields. Table 1 contains the synchrotron integrals [2]. The longitudinal profile of the dipole fringe field reduces the second and the third as well as the fifth synchrotron integrals [3]. Figure 1 shows a half cell in the arc of the damping ring. The dipole field stretches out over the permanent sextupoles to the adjacent quadrupoles. The transverse damping time increases by about 12 % compared to the hard edge model.

The rectangular bending magnets with parallel pole faces cancel the fourth synchrotron integral in the hard edge approximation. For the soft edge model, the fourth synchrotron integral becomes negative, the horizontal damping partition slightly larger than 1.0 and the horizontal damping time is about 1 % shorter than the vertical.

## II. Emittance in the Presence of Misalignments

We have simulated the effects of misalignment errors on the equilibrium emittance and the damping partitions. Random misalignments were generated using gaussian distributions cutoff at $\pm 2\sigma$. Two cases were considered with rms values for the the various elements listed in Table 2. These values are reasonable based on the original design tolerances.
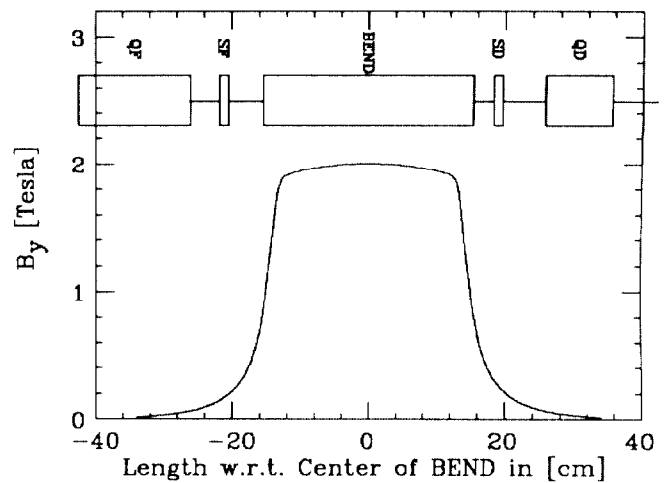


Figure 1: Field of the Main Dipole in a DR Half-Cell

Table 1. Beam parameters for the damping ring without errors and two different fringe field models
Energy = 1.153 GeV

| Characteristic | hard edge model | soft edge model |
|---|---|---|
| $I_2 = \oint G^2 ds$ | 3.2044 | 2.8045 |
| $I_3 = \oint \mid G^3 \mid ds$ | 1.6342 | 1.3595 |
| $I_4 = \oint (G^2 + 2K)G\eta ds$ | -0.0016 | -0.027 |
| $I_5 = \oint \mid G^3 \mid H ds$ | 0.02102 | 0.017482 |
| $J_x = 1 - I_4/I_2$ | 1.0005 | 1.01 |
| $dJ_x/d\delta$ | -14.5 | -14.5 |
| $\epsilon_x$ [nm-rad] | 12.9 | 12.1 |
| $\gamma\epsilon_x$ [$10^{-5}$ m-rad] | 2.88 | 2.73 |
| $\tau_x$ [ms] | 3.40 | 3.84 |
| $\tau_y$ [ms] | 3.40 | 3.88 |
| $U_{rad}$ [keV] | 79.7 | 69.7 |

Table 2: Rms Misalignments Simulated for the NDR.

|  | Case #1 | Case #2 |
|---|---|---|
| Quads $(x, y)$ | 100 $\mu$m | 200 $\mu$m |
| Quads $(\Theta)$ | 0.5 mrad | 1.0 mrad |
| BPMs $(x, y)$ | 100 $\mu$m | 200 $\mu$m |
| Sext $(x, y)$ | 600 $\mu$m | 1000 $\mu$m |

The dependence of the normalized equilibrium emittance on the tune is illustrated in Fig. 2. Here, we have plotted the sum of the transverse normalized emittances, in units of $10^{-5}$ m-rad, versus the fractional tunes; the NDR operates on the difference coupling resonance so the fractional tunes $\nu_x$ and $\nu_y$ are equal. Each data point in Fig. 2 is averaged from 100 simulations of different sets of errors while the error bars correspond to the standard error for each average. In all of the simulations, the orbit was corrected and the path length of the trajectory was adjusted. One can see that the magnitude of the equilibrium emittance increases as the transverse tunes are decreased. This is largely due to the dispersion generated by the alignment errors. The dispersion due to errors is inversely proportional to $\sin \pi\nu$ and thus the increase in emittance should vary as $\Delta\epsilon \propto 1/\sin^2 \pi\nu$. The lines joining the data points in Fig. 2 are fit to this $1/\sin^2 \pi\nu$ dependence.

Unlike the case of the transverse emittances, there was no systematic variation of the damping partitions with either the transverse tunes or the magnitude of the misalignments. The average values for $J_x$ were constant with standard errors of much less than 1%; the fluctuation from seed-to-seed increased with the misalignment magnitude, but, even in Case #2, the rms of the simulated values was less than 4%.
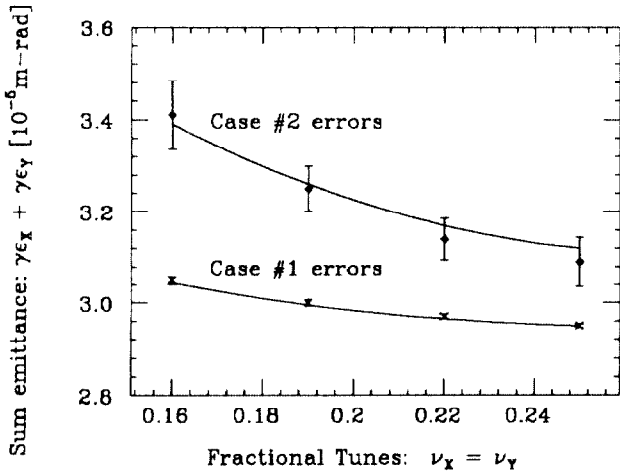


Figure 2: Emittance vs. Tune in NDR Simulations.

The measurements of emittance variations vs. tune were performed after damping the beam for 5.5 ms to increase the observed effect. Assuming no variation of the damping partitions, the variation of the emittance at 5.5ms after injection can be found from:

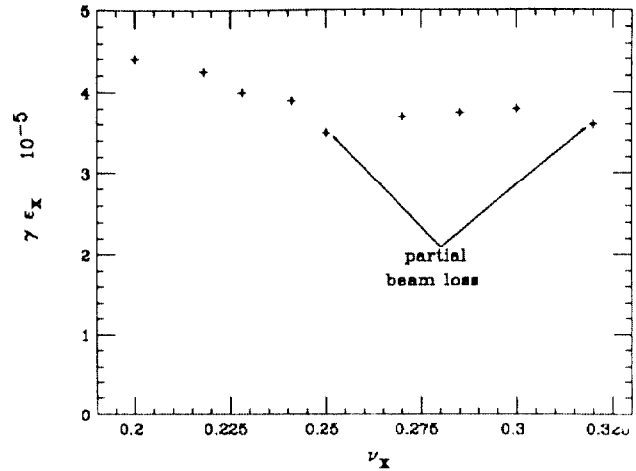$$\Delta\epsilon(t) = \Delta\epsilon_\infty(1 - e^{-2t/\tau}) \quad , \qquad (1)$$



Figure 3: Measured Emittance vs. Tune.

where $\tau$ is the damping time and $\epsilon_\infty$ is the equilibrium emittance; in the NDR, we have $\Delta\epsilon(5.5ms) = 0.94\Delta\epsilon_\infty$. The observed tune variation of the emittance as shown in Fig. 3 (see Ref. [1]) has a behavior similar to that seen in Fig. 2, but the magnitude is larger by a factor of two. This could be explained by assuming larger misalignments; the emittance increase should be proportional to the square of the misalignment magnitude. Alternately, one could assume that we have a bad misalignment 'seed' in the NDR. The rms of the simulated values is roughly a factor of 10 larger than the standard errors. Thus, the rms of the emittances values simulated in Case #2 is almost $\Delta\gamma\epsilon_{sum} \sim 1 \times 10^{-5}$ m-rad. Since the distribution for the emittance increase is approximately exponential [5], there is a 5% probability that the emittance increase from any specific seed can exceed the average value by three times this rms value.

### III. SYNCHRO - BETATRON COUPLING

Both damping rings have been designed without dispersion suppressors so that the horizontal dispersion does not cancel in the two RF cavities. The radiation lost in the arcs is replaced in the cavities within a distance short
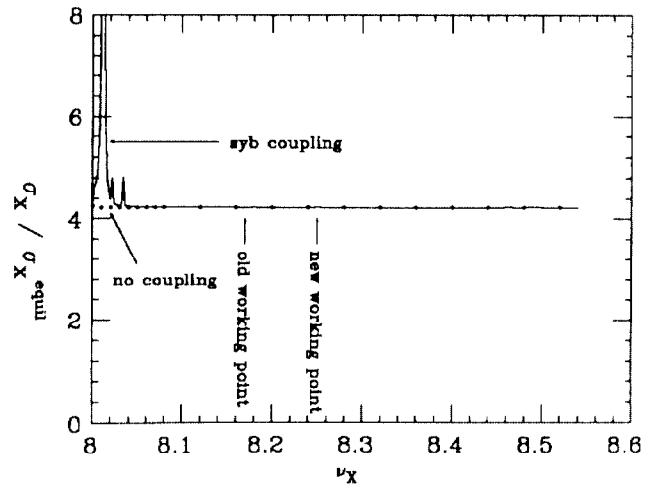


Fig. 4 Synchro-betatron excitation of the beam size

compared to the betatron wavelength so that the betatron coordinate is shifted by:

$$\delta x = -\eta_x \Delta\epsilon = -\eta_x \frac{eV_{RF}}{E_0}\left[\sin(\phi_s - 2\pi z f_{RF}/c) - \sin(\phi_s)\right]$$

We use the coordinates $(x, x', z, \epsilon)$ to describe the evolution of an individual particle w.r.t. the bunch center. $V_{RF}$ is the peak voltage provided by the cavity and $\phi_s$ is the synchronous phase. In the cavity the longitudinal position couples to the transverse betatron motion. But also the longitudinal motion is affected by the transverse motion: A betatron oscillation will change the path length over the arc [6]:

$$\Delta z = -\int_{ARC} G(s)(x + \eta_x \epsilon)ds ,$$

where $G(s)$ denotes the local curvature. The one turn map consists of a five sequential transformations:

$$\begin{pmatrix} U_{ARC} \\ \to \end{pmatrix}\begin{pmatrix} U_{RF1} \\ \to \end{pmatrix}\begin{pmatrix} U_{ARC} \\ \to \end{pmatrix}\begin{pmatrix} U_{RF2} \\ \to \end{pmatrix}\begin{pmatrix} U_{DAMP} \\ \to \end{pmatrix}$$

and $U_{DAMP}$ should reproduce the expected damping of the emittance as a function of turns $n$:

$$\epsilon_n = (\epsilon_i - \epsilon_\infty)e^{-2nT_0/\tau} + \epsilon_\infty .$$

250 particles have been simulated at the tunes $\nu_x = 8.17$ over 50000 turns which correspond to 5.5 ms of store time in the damping ring. No blow up of the beam size could be seen. We also investigated a possible effect at lower tunes and found the excitation of synchrotron sidebands due to the non-linear field of the RF cavity, but no effect above $\nu_x = 8.10$. Figure 4 shows the simulated blow up of the beam size after 4800 turns.

The results agree well with an analytic approximation for the beam size blow up due to synchro - betatron coupling far from resonance as derived in Ref. [7]. Because the synchrotron tune is small, $\nu_s \approx 0.01$, the dominant contribution comes from the first-order resonance; the higher-order resonances are too narrow to have a significant effect.

Finally, it is important to note that synchro-betatron coupling can also be induced by transverse and longitudinal wakefields. But, this effect should depend on the bunch charge and on the orbit in the RF cavity, which has not been observed [1].

## CONCLUSIONS

The calculated damping times are in good agreement with our measurements if a realistic model for the longitudinal field distribution of the bending magnets is used. A remaining small difference ($\approx 10\%$) may be attributed to a systematic orbit offset due to a misalignments of the magnet support girders. The observed tune dependence of the emittance can be explained with the tune dependence of the spurious dispersion generated by magnet misalignments. Synchro-betatron coupling, a likely suspect since the dispersion in the damping ring RF cavities is not zero, was ruled out as a reason for a significant emittance increase in the tune range in question.

## REFERENCES

[1] F. J. Decker et al., Measured Emittance versus Store Time, contribution to this conference .

[2] R. Helm et al., IEEE Trs. Nucl. Sci. 20, 900, 1973.

[3] J. P. Delahaye, L. Rivkin, IEEE Trs. Nucl. Sci. 32, 1695, 1985.

[4] L. Sagalovsky, Nucl. Instr. Meth. A298, 205, 1990.

[5] T. Raubenheimer, Tolerances to Limit the Vertical Emittance in Future Storage Rings, SLAC-PUB-4937, 1991.

[6] A. Piwinski et al., Excitation of Betatron-Synchrotron Resonances DESY-76/07, 1990.

[7] T. Raubenheimer, Ph.D. Thesis, SLAC-387, 1991.